Revista Mexicana de Astronomía y Astrofísica, **44**, 57–70 (2008)

DETERMINATION OF THE IMF IN THE LMC STELLAR CLUSTER NGC 2156

E. Silva-Villa,[1,2] M. Sirianni,[1,3] and J. Zuluaga[2]

Received 2007 August 15; accepted 2007 October 23

RESUMEN

Presentamos un estudio de la IMF del cúmulo estelar NGC 2156 de la LMC usando imágenes tomadas por el telescopio espacial Hubble en las bandas F555W y F814W. El estudio forma parte de un programa dedicado a investigar si la IMF para estrellas de baja masas es dependiente de las condiciones locales, observando cúmulos jóvenes en la LMC y SMC. Hemos detectado estrellas hasta una magnitud límite de $m_{555} = 26$, correspondiente a una masa estelar de $\sim 0.6 M_{\odot}$ a la distancia de la LMC (50.11 Kpc). La comparación de los diagramas CMD con isocronas teóricas indica una edad de 49 ± 5 Myr para este cúmulo. Se realizó un análisis de completitud y una determinación de la contaminación de estrellas de fondo para corregir la LF y así derivar la MF del cúmulo, usando la relación ML estándar para estrellas de la secuencia principal. Dado que el cúmulo es muy joven, la MF observada es una buena aproximación a la IMF.

ABSTRACT

We present a study on the IMF of the stellar cluster NGC 2156 in the LMC from deep HST-WFPC2 images in the bands F555W and F814W. The study is part of a larger program to investigate whether the IMF at low stellar masses is dependent on local conditions by observing young globular clusters in the LMC and the SMC. We detected stars down to a limiting magnitude of $m_{555} = 26$, which corresponds to stellar masses of $\sim 0.6\ M_{\odot}$ at the distance of the LMC (50.11 Kpc). A comparison of the cluster CMD with theoretical isochrones indicates an age of 49 ± 5 Myr. We performed a completeness analysis and determined the background stellar contamination to correct the observed LF and derive the MF of the cluster using the standard ML-relation for main sequence stars. Given the fact that the cluster is very young, the present day MF is expected to be a good approximation to the IMF.

Key Words: methods: data analysis — stars: formation — stars: low-mass — stars: luminosity function, mass function — techniques: image processing

1. INTRODUCTION

Since the seminal paper by Salpeter (1955) about the Initial Mass Function (IMF) of the solar neighborhood, many authors have been studying the stellar IMF in the field and in open stellar clusters in our Galaxy. The study of the IMF, normally in relation to galactic field stars and stellar clusters, has become a leading field in stellar evolution research. In most cases the IMF seems to be well described by a power law, with a constant slope approximately equal to the value derived by Salpeter ($\Gamma = -1.35$). Slightly different slopes in different mass intervals are also observed (see Figure 1). The IMF for field stars and young stellar clusters exhibits for example a unique set of features in the mass range 1–15 $M_{\odot}$.

During the last two decades the IMF at low stellar masses has received special attention. At those masses a wider range of values for Γ has been found. There the IMF is steeper than for intermediate and high stellar masses.

In the 1950's, van den Bergh (1957) questioned the universality of $\Gamma = -1.35$ performing a study

[1]Space Telescope Science Institute, Baltimore, USA.

[2]Instituto de Física, Universidad de Antioquia, Medellín, Colombia.

[3]Science Operation Development Division, European Space Agency, The Netherlands.

over 20 clusters, where he found differences in the IMF for low mass stars. Although his work had recognised completeness problems, he left open the question about the universality of the IMF.

On the other hand, if the IMF is found to be universal new theoretical and observational issues must be addressed: (1) How can the complexity of the stellar formation process yield a universal IMF? (2) Are the observations consistent with the universal IMF hypothesis simply because the current uncertainties in the empirical estimates are very large? (Kennicutt 1998).

The universality of the IMF has been questioned by studies in two types of stellar systems:

- *Field stars.* Initial studies of the IMF of field stars deviated from the original value found by Salpeter's study. Scalo (1986) found $\Gamma = -2.6$ for stars in the $1.4 - 3.5\ M_{\odot}$ mass range. Kroupa, Tout, & Gilmore (1993) performed a more extended fit over the data used by Scalo in the full range of masses above 1 $M_{\odot}$ and found $\Gamma = -1.7$.

- *Stellar clusters.* The study of the IMF of stellar clusters provides a fundamental piece of evidence to the universality hypothesis. Stars in a cluster are formed approximately at the same time and with similar chemical composition. However IMF studies in stellar clusters are affected by several important factors, e.g., the lack of a sufficiently wide range of masses and ages, effects like mass segregation or field star contamination, uncertainties in the composition of binary systems, distance, metallicity, extinction and differential reddening, etc. All these factors have an effect on the derived IMF.

  The IMF in clusters has been studied since 1957 (van den Bergh 1957). Typical slope values were obtained by Scalo (1986), Taff (1974) $\Gamma = -1.7$, Claudius & Grosbol (1980) $-1.6 < \Gamma < -2$ and Tarrab (1982) $-1 < \Gamma < -2$, among others.

In order to derive the mass function (MF) from the observed luminosity function (LF) an accurate Mass-Luminosity relation (MLR) is required. The MLR is especially important for low mass stars (Kroupa, Tout, & Gilmore 1990; Kroupa et al. 1993; D'Antona 1998) and its uncertainty has an important impact on the IMF for this range of masses. High precision surveys performed in the last decades exploring the low mass region (below 4 $M_{\odot}$) have improved the understanding of the MLR.

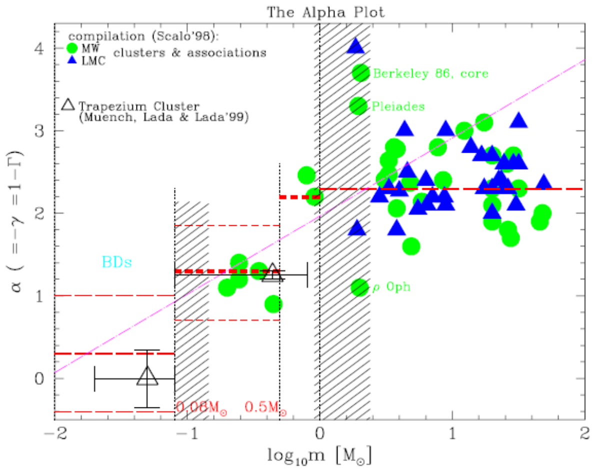

Fig. 1. The α-plot for stellar clusters and associations in the Magellanic Clouds and in our Galaxy created by Kroupa (2001). Data are taken from Scalo (1998). The horizontal dashed lines are the average IMF with estimated uncertainties (equation 2 in Kroupa 2001), and the diagonal dot-dashed line is the classical IMF (Miller & Scalo 1979).

Many of the uncertainties of Γ are due to differences in the methods used for data analysis and in particular to the MLR and theoretical isochrones adopted (Massey 2003). In 1993 Phelps studied the IMF of NGC 663 and NGC 581, two clusters with similar ages and populations (Phelps & Janes 1993), and found very different values for the IMF slopes: $\Gamma = -1.1$ for NGC 663, and $\Gamma = -1.8$ for NGC 583, even though the data reduction process was identical for both clusters. Many other authors have found IMF slopes as steeper as -2 for masses in the range $1 - 10\ M_{\odot}$ (see for example Prisinzano et al. 2003; Sanner & Geffert 2001; Kalirai et al. 2003; Prisinzano et al. 2001; Sagar, Munari, & de Boer 2001) and others have measured even flatter IMF, $\Gamma \sim -0.9$, (see for example Scalo 1998; Sung & Bessell 2004). Intermediate slopes consistent with Salpeter's value have also been found $-1.1 < \Gamma < -1.6$ (see for example Sanner & Geffert 2001; Yadav & Sagar 2002, 2004).

As part of a larger program aimed at determining the impact of differences in local environment on the IMF of young stellar clusters in the Large and Small Magellanic Clouds (LMC and SMC respectively), we have studied and analyzed deep *Hubble Space Telescope* (HST) images of the star cluster NGC 2156 in the LMC using the *Wide Field Planetary Camera 2* (WFPC2). Globally the idea is to study a large sample of clusters so as to try to reduce the particular uncertainties related to the data reduction and analysis.

This paper has the following structure: in § 2 we present the star cluster target of our study; § 3 presents details about the observational data and their analysis; §§ 4 and 5 are devoted to the stellar photometry and the age estimation respectively; finally in §§ 6 through 8 we present the completeness analysis, the derivation of the luminosity and mass functions and the discussion and conclusions related to our results.

2. NGC 2156

The stellar cluster NGC 2156 is one of the youngest clusters of the LMC halo. The cluster is located in the southwest region of the galaxy with coordinates $\alpha : 05^h57^m$ and $\delta : -68°27'$ (J2000.0) (Bica et al. 1999). The first age estimation of this cluster was made by Elson (1991), who estimated that NGC 2156 was 39.8 ± 1.6 Myr old.

The two main components of the LMC, bar and disc, present marked differences in the age distribution as shown by Smecker-Hane et al. (2002). The LMC bar has an age in the range of 1–6 Gyr while in the disc, the star formation process has been relatively continuous over the last ~ 15 Gyr. This age difference, known as the age gap of the LMC, is believed to be the result of the gravitational interaction with the SMC and the Milky-Way (MW) (Smecker-Hane et al. 2002).

NGC 2156 is an ideal case for IMF studies because of its young age. The measurement of its Mass Function (MF) is a direct indicator of its original IMF. Deep images of the cluster allow the study of stellar masses below $M \sim 1\ M_\odot$. The metallicity of the cluster has not been previously measured so for the purpose of this work we will use a metallicity of $Z = 0.008$.

3. OBSERVATION AND DATA REDUCTION

The images of NGC 2156 were taken centering the *Planetary Camera* (PC) of the WFPC2 on board of the HST on the core of the cluster while the *Wide Field Cameras* (WFs) imaged the outer regions (see Figure 2). The PC has a field-of-view (FOV) of $34'' \times 34''$ and a resolution of $0.046''$ per pixel while the WFs has a FOV of $75'' \times 75''$ and a resolution of $0.1''$ per pixel.

Four long exposure images (exptime = 350 s) and one short exposure image (exptime = 10 s) were taken in two bands, F555W ($\sim V$) and F814W ($\sim I$). Table 1 summarizes the journal of the observations.

The data were processed adopting the standard STScI pipeline, which uses calibration observations and reference data such as bias, flat-field, and dark frames that are constantly updated by the STScI WFPC2 team to track any changes in the performance of the camera and its detectors. The basic steps of the calibration include the correction for the errors introduced by the analog to digital conversion, the removal of the bias level and bias pixel-to-pixel variations, the dark subtraction, and the flatfield application, among others. The individual images were stacked together to remove cosmic-ray contamination.

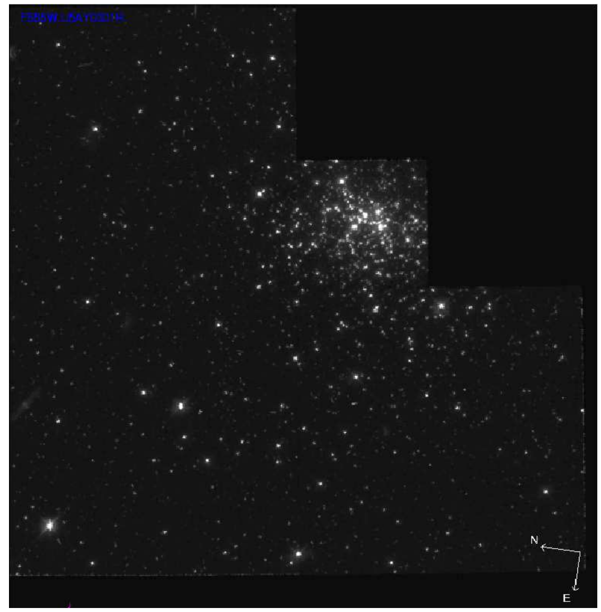

Fig. 2. Combined images of NGC 2156 for the 4 cameras using HST-WFPC2.

4. PHOTOMETRY

The photometry of NGC 2156 was performed following the methodology used by Sirianni et al. (2000) to perform the analysis of NGC 330.

In our long expoures, many stars were completely saturated. Short exposures were used to obtain the precise position and magnitude of the saturated stars.

A statistical analysis over a sample of bona fide stars selected over the images was performed to properly select the DAOFIND parameters, i.e. roundness and sharpness. Still, DAOFIND returned several spurious objects that we removed manually after a careful inspection.

We found a total of 1226 stars in the PC camera and 4314 in the WFs.

After running aperture photometry and PSF fitting photometry we compared the results obtained

TABLE 1

JOURNAL OF HST-WFPC2 OBSERVATIONS OF NGC 2156

Proposal	Date	Filter	Exp Time (s)	Image name
NGC 2156 (J2000.0) $\alpha : 05^h57^m54^s.33$ $\delta : -68^o27^{'}20^{''}.02$				
8134	1999 Aug 22	F555W	350	u5ay0301r
8134	1999 Aug 22	F555W	350	u5ay0302r
8134	1999 Aug 22	F555W	10	u5ay0303r
8134	1999 Aug 22	F814W	350	u5ay0304r
8134	1999 Aug 22	F814W	350	u5ay0305r
8134	1999 Aug 22	F814W	10	u5ay0306r
NGC 2156 (J2000.0) $\alpha : 05^h57^m54^s.38$ $\delta : -68^o27^{'}20^{''}.0$				
8134	1999 Aug 22	F814W	350	u5ay0307r
8134	1999 Aug 22	F814W	350	u5ay0308r
8134	1999 Aug 22	F555W	350	u5ay0309r
8134	1999 Aug 22	F555W	350	u5ay030ar

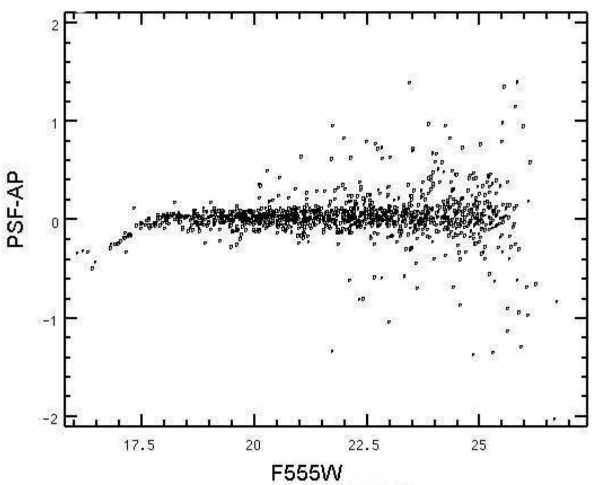

Fig. 3. Comparison of the magnitudes obtained with PSF and AP vs. $m_{\rm F555W}$. The data correspond to long exposure images taken with the PC.

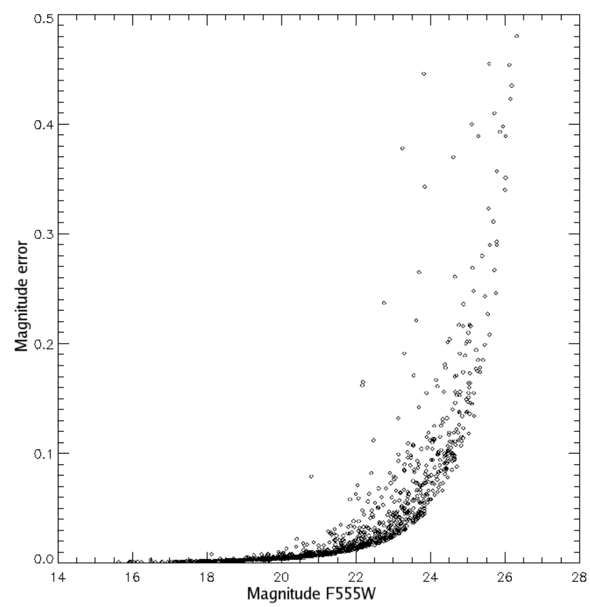

Fig. 4. $\sigma_{\rm AP}$ vs. $m_{\rm F555W}$ (long exposure, PC).

for the stellar magnitudes as shown in Figure 3 and no systematic differences were observed.

Analysing the photometric errors (Figures 4 and 5) we see that for aperture photometry the uncertainty grows steeply for faint stars ($m_{\rm F555W} \geq 23$) while in the case of PSF fitting the error is smaller than $\sigma_{\rm PSF} = 0.2$ for bright and faint stars. Since we are interested in the study of low-mass stars, we decided that PSF fitting is the most accurate photometry method for the purpose of this work.

The PSF fitting routine returned 1183 and 4062 stars for the PC and WFs respectively.

The instrumental magnitudes ($m_{\rm instr}$) have to be converted to real magnitudes (m) by removing instrumental effects. As usual the total counts were corrected for exposure time and aperture correction. A special correction was required to take into account, the *Charge Transfer Efficiency* (CTE) degradation (Dolphin 2000). This effect is due to the partial loss of signal when charge is transferred down the chip during the readout operation, with the consequence that stars at higher row numbers appear

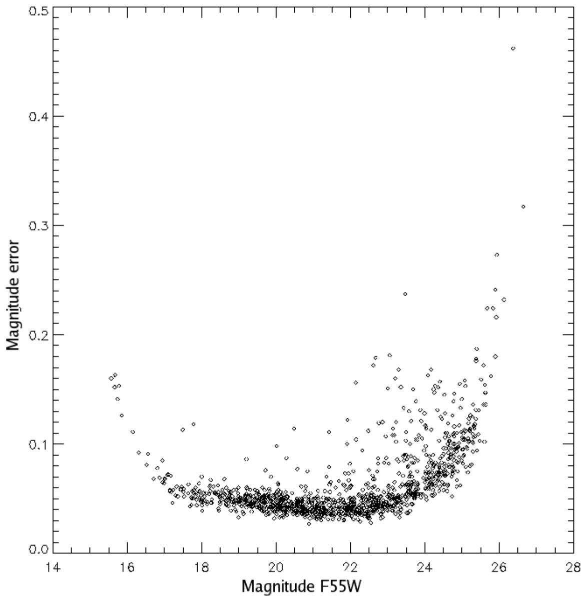

Fig. 5. $\sigma_{\rm PSF}$ vs. $m_{\rm F555W}$ (long exposure, PC).

fainter than they would if they were at low row numbers (Holtzman et al. 1995). Finally we adopted the zero points derived by Dolphin (2000). The resulting formula for the real magnitude is:

$$\begin{aligned} m &= m_{\rm instr} + 2.5\log({\rm t}) \\ &\quad + m_{\rm HST} - {\rm AP_{corr}} - {\rm CTE} \end{aligned} \tag{1}$$

where $m_{\rm HST}$ is the zero point, $\rm AP_{corr}$ is the aperture correction and t the exposure time.

5. COLOR-MAGNITUDE DIAGRAMS AND AGE ESTIMATION

With the corrected stellar magnitudes we constructed the Color-Magnitude Diagram (CMD) for the cluster. Only those stars with a photometry accuracy better than ($\sigma_{\rm PSF} \leq 0.2$) in both filters were used in this analysis.

Three different sets of stars were used to construct the CMDs: non-saturated and faint stars from the long exposure images ($m \geq 19.5$) and bright but non-saturated stars ($18 \leq m \leq 19.5$) common in both exposures. Stars saturated in the long exposure were measured in the short exposure images ($m \leq 18$).

We assumed an extinction $A_v = 0.31$ (Elson 1991) and a metallicity $Z = 0.008$. The best fit to the main sequence and turn-off-point of our CMD was found by computing a least-square statistics using the theoretical isochrones from Lejune & Schaerer (2001).

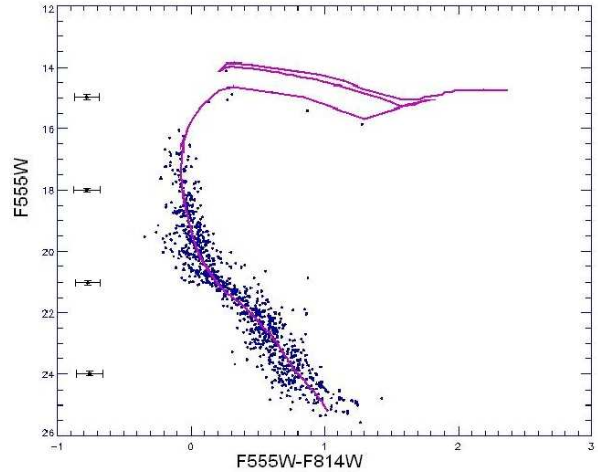

Fig. 6. Color-Magnitude diagrams for the PC and best fit theoretical isochrone from Lejune & Schaerer (2001).

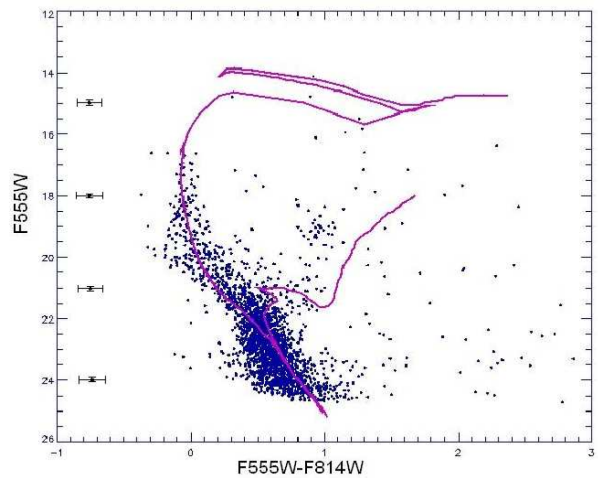

Fig. 7. Color-Magnitude diagram for the WFCs and best fit theoretical isochrone from Lejune & Schaerer (2001).

In order to avoid the field star contamination in estimating the age of the cluster only stars in the PC camera were initially taken into account (see Figure 6). We estimate an age of 49 ± 5 Myr for the cluster, in agreement with previously published results (Elson 1991).

Considering the CMD of peripheral stars in the image (stars mainly in the WFCs) a second turn-off point (TO) is observed (see Figure 7). This additional TO arises from the presence of older field stars that do not belong to the cluster but to the LMC. To verify the accuracy of our procedure we also fitted isochrones on the CMD of these field stars. Assuming the same metallicity as before, and using an extinction of $A_v = 0.25$, we estimated an age of 2.5 Gyr

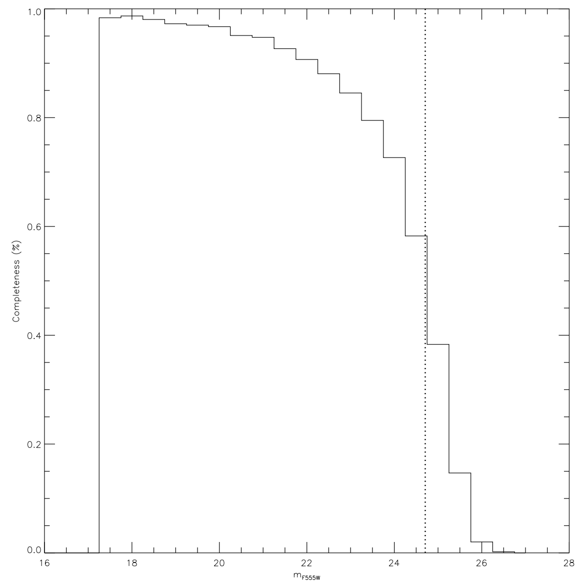

Fig. 8. Completeness diagram for the filter F555W. The vertical dotted line is the 50% completeness limit.

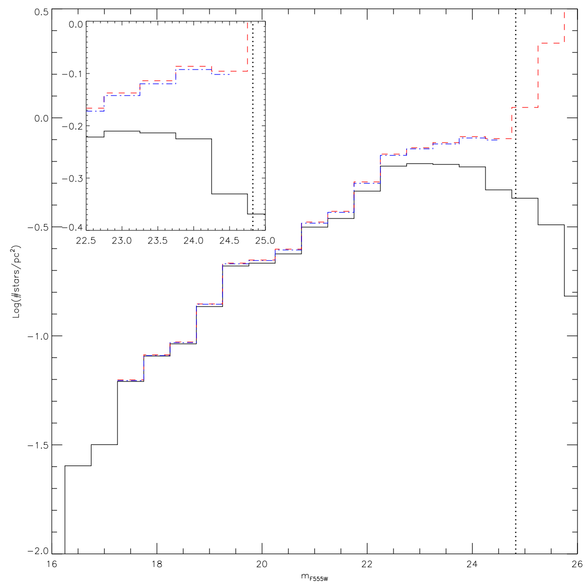

Fig. 9. Luminosity function for NGC 2156. The solid line shows the observed LF, the dashed line shows the completeness-corrected LF and the dash-dotted line shows the LF corrected for completeness and background contamination. The 50% completeness is the vertical dotted line. A zoom has been overplotted to show the small corrections found.

in good agreement with previously published results (Smecker-Hane et al. 2002) for the age of the field stars in the bar of the LMC.

6. COMPLETENESS AND SURFACE STELLAR DENSITY

Completeness

Before deriving the IMF we need to assess the completeness of our data. Artificial stars were added to the image for each half magnitude bin. The number of artificial stars was less than 5% of the total number of stars in order to avoid impacting the star density of the image. Then we tried to retrieve the artificial stars using the same selection and photometry parameters used on the original images. These tests were run 100 times every 0.5 magnitudes. The completeness was found to be better than 50% up to $m_{\rm F555W} = 24.7$. Figure 8 presents the completeness diagram resulting from this analysis.

Surface Stellar Density

In order to obtain a normalized LF we computed the average stellar density on annuli of 10 arcsec in width from the center of the cluster to the outer regions. The area of each annulus was obtained using a simple Monte Carlo procedure. A fixed number of points (N_{mc}) was uniformly sampled over the total surface of the image. The area of a given annulus was computed from the number of points (N_a) that fell inside that annulus using the equation $s = N_{mc}/N_a \times N_s/A_t$, with A_t being the total area of the image.

7. LUMINOSITY FUNCTION AND MASS FUNCTION

Luminosity Function (LF)

The LF, star density per unit of magnitude and unit of area, was obtained by counting the number of stars in each magnitude bin in a given region of the image (the annuli or the total image) divided by the magnitude bin width and the area of the selected region. The resulting LF is shown in Figure 9. The observed LF must then be corrected for completeness.

Figure 7 shows significant contamination from stars that do not belong to the cluster but rather to the LMC field. We calculated the background contamination by deriving the LF for the field stars. A study of the slope in the LF corrected for completeness was performed from the core of the cluster to the outer regions every 10 arcsecs. The slopes of the LF were found using a linear fit minimizing the χ^2-error statistic. Starting from the center of our cluster and going to the outer regions, the slope of the LF grows until it stabilizes (see Figure 10). The result of this test was that

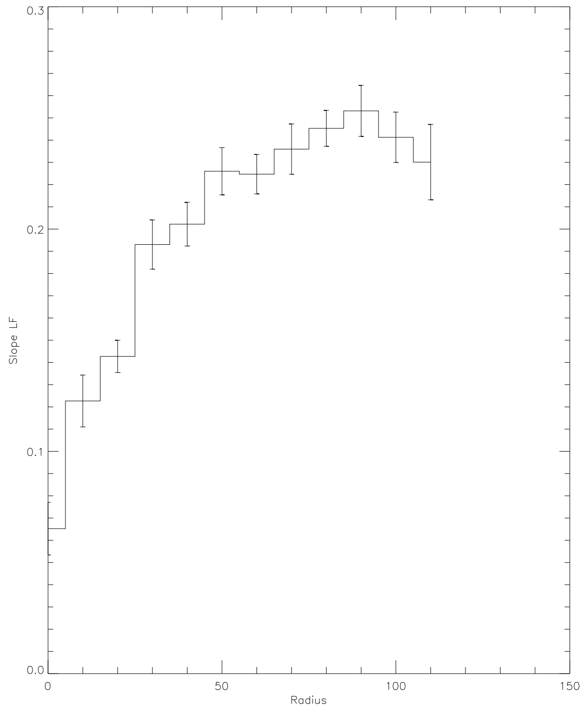

Fig. 10. Radial distribution of the slope of the luminosity function from the center of the cluster to the outer regions. We assumed a background LF for the region beyond 95″.

regions external to $r \geq 95''$ probably contain more stars from the LMC field than from the cluster. We assume that the observed LF of this outer region is that of the background and correct the LF of the inner parts by subtracting it (see Figure 9 dash-dotted line).

Mass Function (MF)

The conversion of the LF to the MF is achieved using the formula:

$$MF = LF \times \left| \frac{\partial m}{\partial \log M} \right| \qquad (2)$$

The MLR was derived using the isochrone that best fit our CMD with the procedures described by Tarrab (1982). In Table 2 we present the results of this analysis which were used to obtain the MF's depicted in Figure 11.

The observed MF and the one corrected for completeness and background contamination is shown in Figure 11. The best fit line in the log-log yields a value for the exponent $\Gamma = -1.69 \pm 0.13$ for the mass range $1.2 < M/M_{\odot} < 6.3$, which is in good agreement with the typical value derived for the LMC clusters (Kroupa & Boily 2002).

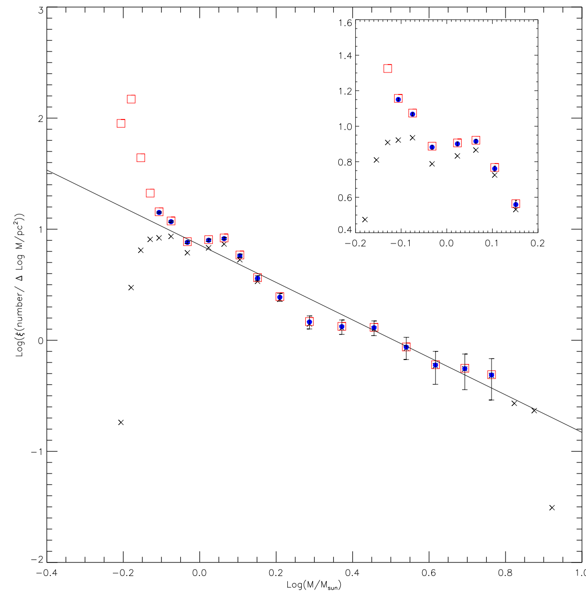

Fig. 11. Mass Function for NGC 2156. Observed MF (x), completeness-corrected MF (*squares*), MF corrected for completeness and background contamination (•) and the best fit approximation (solid line). A zoom has been overploted to show the small corrections found.

The good statistics of our sample give us an opportunity to study the behavior of the MF at different radii (see Figure 12). To do this, we computed the relevant quantity in 14 annuli starting from the central region to the outer part of the cluster (130″). The results are shown in Figures 13 to 17. A more detailed disscussion about this radial study is presented in the next section.

8. DISCUSSION AND CONCLUSIONS

We have presented a detailed study of the LMC cluster NGC 2156. Our main goal was the study the IMF for the low-mass range.

Our estimated age of NGC 2156 is 49 ± 5 Myr which is slightly higher, but still in agreement with previous estimations. Given the moderately young age, the present day mass function is still a good represntation of the IMF for star still in the MS.

The IMF obtained from these analysis has a slope of $\Gamma = -1.69 \pm 0.13$ which is in good agreement with the value obtained for other LMC clusters in the mass range $1.2 < M/M_{\odot} < 6.3$.

We also performed a radial analysis of the mass function. This study shows a variation in the slope of the IMF as we move outwards in the cluster. This variation is likely to be produced by two physical effects:

TABLE 2

TABLE WITH THE THEORETICAL VALUES USED TO CONVERT THE LUMINOSITY FUNCTION INTO A MASS FUNCTION

Luminosity	$\mathrm{Temperature}_{\mathrm{eff}}$	m_{F555W}	$\mathrm{Color}_{\mathrm{theory}}$	Mass	Derivative
2730.75	21029.9	16.7964	−0.232984	7.	−8.79207
1425.16	20041.	17.385	−0.221432	6.	−8.03515
699.781	18509.7	17.9613	−0.202091	5.	−6.8653
303.468	16528.9	18.5866	−0.174083	4.	−6.34892
102.473	14077.8	19.3669	−0.134168	3.	−6.08808
52.0633	12620.4	19.8365	−0.105961	2.5	−5.98873
32.051	11642.2	20.1722	−0.0828289	2.2	−5.98404
22.199	10891.3	20.4173	−0.0604774	2.	−5.90773
18.1556	10478.7	20.5486	−0.0452493	1.9	−5.89198
14.6405	10035.	20.6869	−0.0241517	1.8	−6.30466
11.6419	9558.	20.8537	0.00666473	1.7	−6.85399
9.08144	9052.07	21.0377	0.0532314	1.6	−7.57397
6.93953	8518.07	21.2664	0.124974	1.5	−8.77214
5.17111	7957.08	21.5476	0.23313	1.4	−10.0412
3.73384	7380.12	21.8919	0.373521	1.3	−11.2835
2.59021	6891.03	22.3045	0.476478	1.2	−12.1733
1.72042	6511.15	22.776	0.557405	1.1	−12.3086
1.11676	6189.91	23.2785	0.628138	1.	−9.46282
0.868634	5901.91	23.589	0.694788	0.9	−10.2645
0.498302	5309.03	24.292	0.851713	0.8	−17.442
0.225243	4550.77	25.518	1.15992	0.7	−20.022
0.111901	3989.15	26.7835	1.52865	0.6	−18.9031

- *The LMC Field Stars*

  The field covered by the WF cameras of HST-WFPC2 did not include enough LMC stars to sample the background contamination. The lack of enough field stars was reflected as a small correction in the IMF (see zooms in Figures 9 and 11).

  A better estimate of the background contamination should be done using a more external field.

- *Mass Segregation*

  Through repeated stellar encounters the stars in the cluster approach energy equipartition, inducing more massive stars to give part of their kinetic energy to lighter objects and to sink deeper into the cluster's potential well. Light stars on the other hand, can diffuse outward, passing onto larger, more energetic orbits.

Both phenomena are evident in the shape of the radial distribution of the IMF slopes (see Figures 13–17). The first effect creates a shallower IMF, because if the background contamination contains many cluster stars, then there is an over-correction in the number of low-mass stars in the cluster's core; the latter

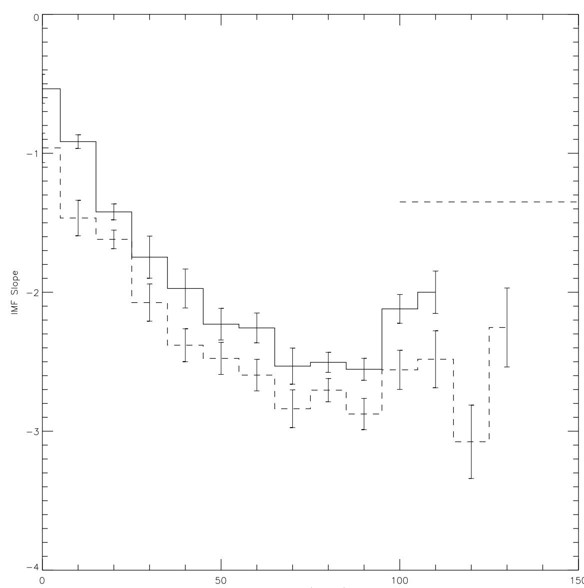

Fig. 12. Radial variation of the initial mass function slope for the stellar cluster NGC 2156. IMF corrected for completeness (*dashed line*). IMF corrected for completeness and background contamination (*solid line*).

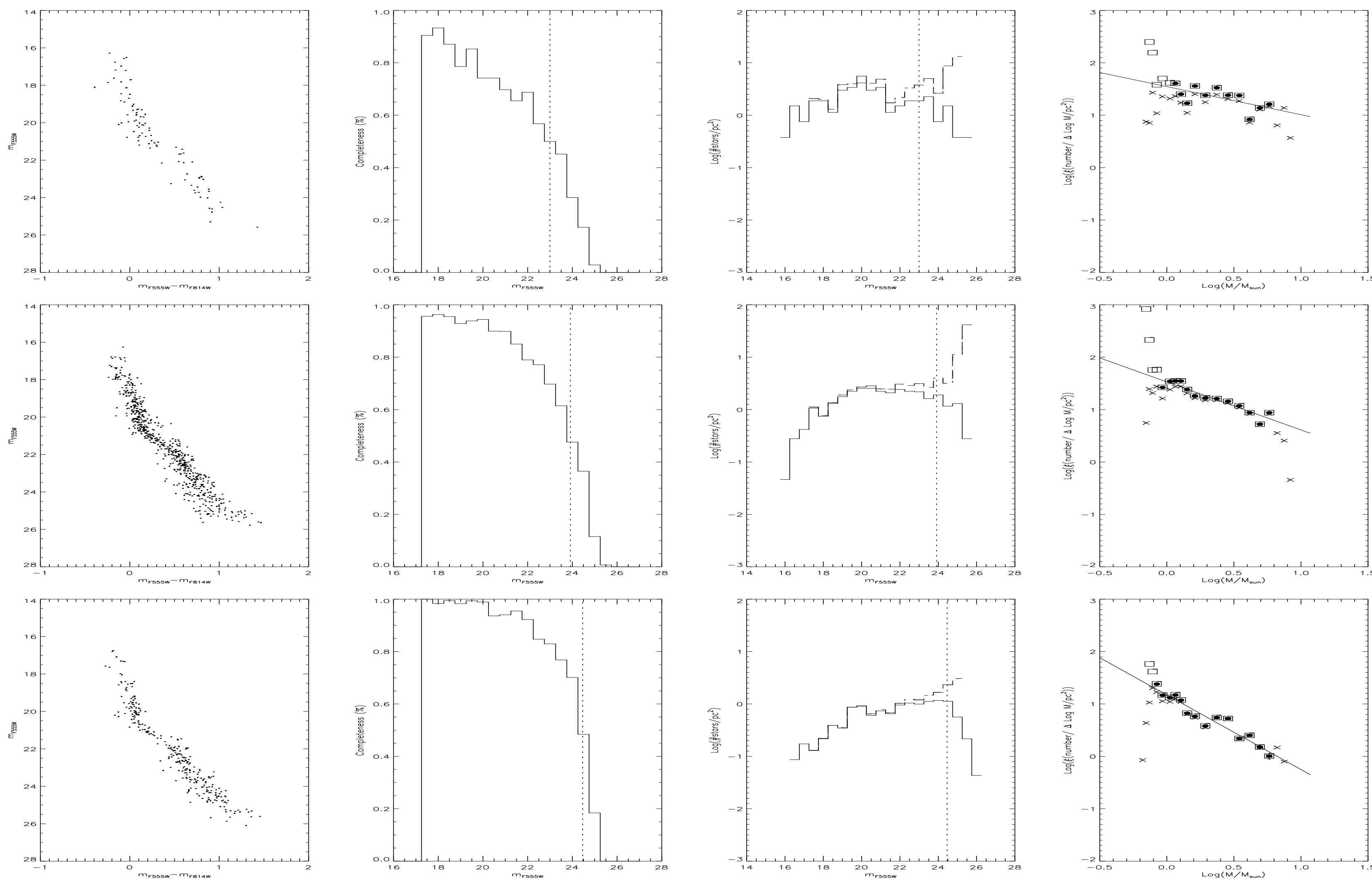

Fig. 13. Diagrams for stars between 0 and 20 arcsec. Each row represents annuli of 10″. Columns: (a) CMDs for main sequence stars; (b) Completeness diagrams (solid line) and magnitude level for 50% completeness (vertical dotted line); (c) Observed LF (solid line), completeness-corrected LF (dashed line) and background-corrected LF (dash-dotted line) and magnitude level for 50% completeness (vertical dotted line); (d) Observed MF (x), completeness-corrected MF (*squares*), background-corrected MF (•) and best fit approximation (solid line).

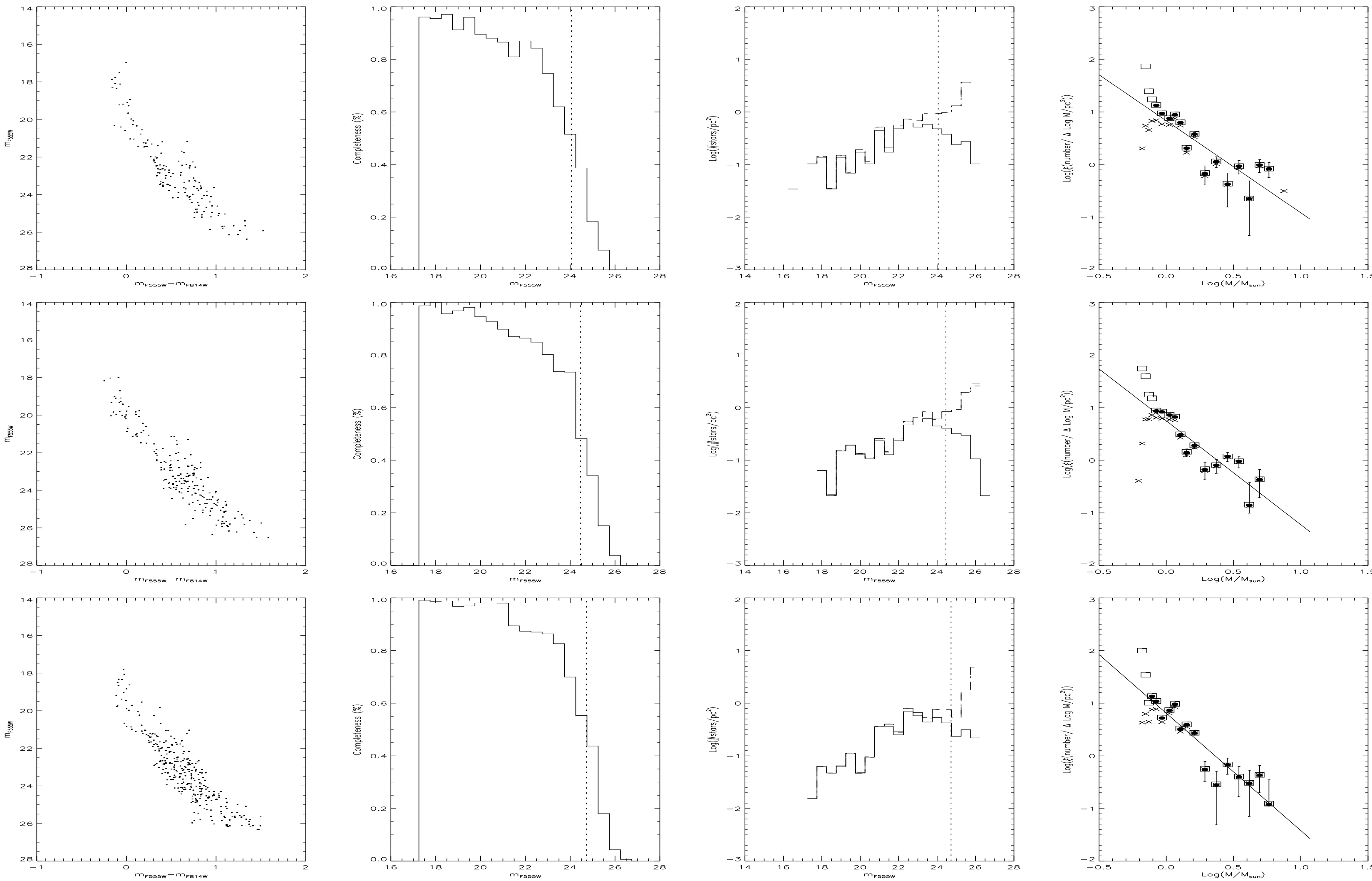

Fig. 14. Diagrams for stars between 30 and 50 arcsec. Each row represents annuli of 10″. Columns: (a) CMDs for main sequence stars; (b) Completeness diagrams (solid line) and magnitude level for 50% completeness (vertical dotted line); (c) Observed LF (solid line), completeness-corrected LF (dashed line) and background-corrected LF (dash-dotted line)and magnitude level for 50% completeness (vertical dotted line); (d) Observed MF (x), completeness-corrected MF (*squares*), background-corrected MF (•) and best fit approximation (solid line).

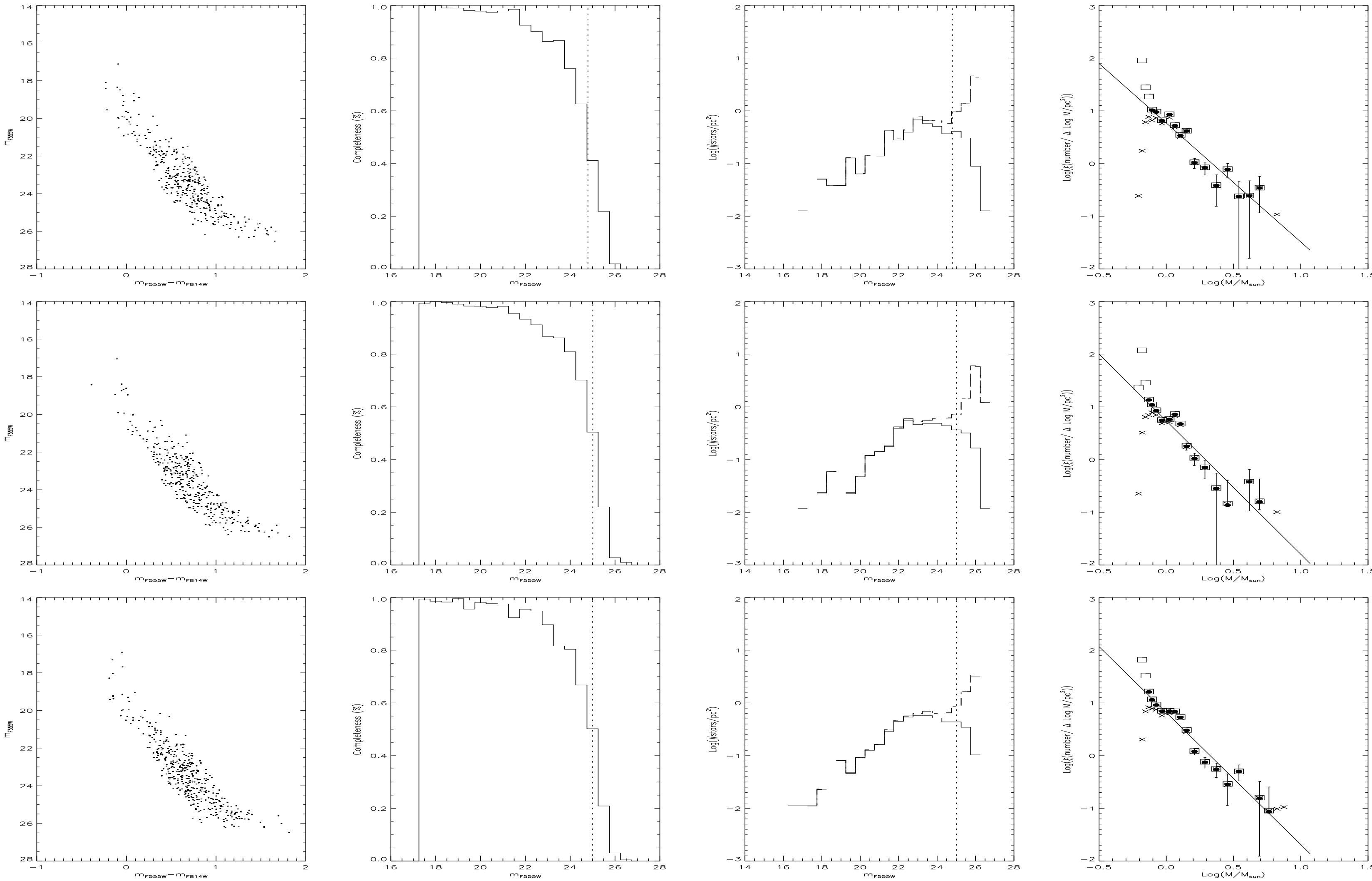

Fig. 15. Diagrams for stars between 60 and 80 arcsec. Each row represents annuli of 10″. Columns: a) CMDs for main sequence stars; b) Completeness diagrams (solid line) and magnitude level for 50% completeness (vertical dotted line); c) Observed LF (solid line), completeness-corrected LF (dashed line) and background-corrected LF (dash-dotted line)and magnitude level for 50% completeness (vertical dotted line); d) Observed MF (x), completeness-corrected MF (*squares*), background-corrected MF (•) and best fit approximation (solid line).

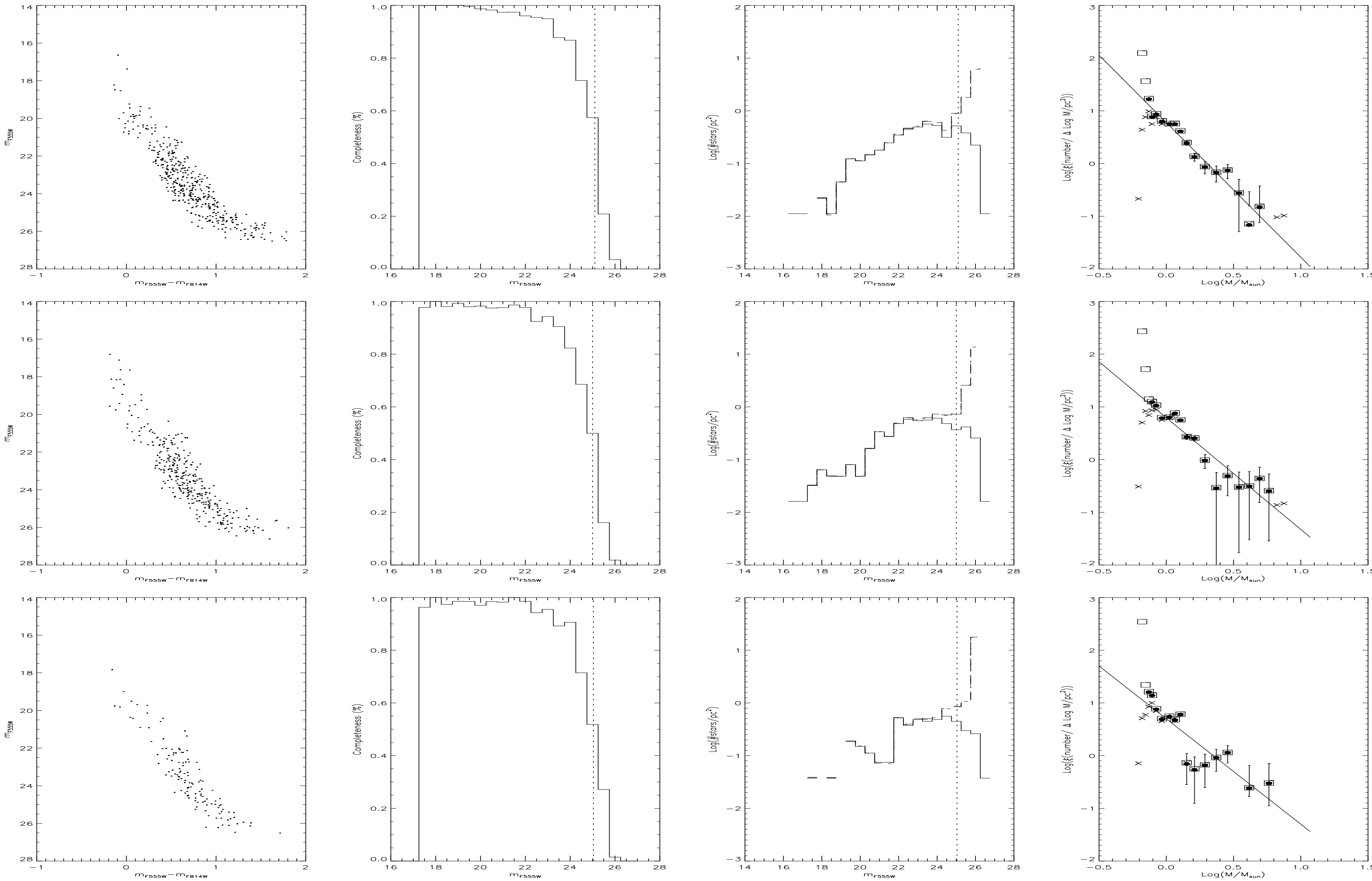

Fig. 16. Diagrams for stars between 90 and 110 arcsec. Each row represents annuli of 10″. Columns: (a) CMDs for main sequence stars; (b) Completeness diagrams (solid line) and magnitude level for 50% completeness (vertical dotted line); (c) Observed LF (solid line), completeness-corrected LF (dashed line) and background-corrected LF (dash-dotted line)and magnitude level for 50% completeness (vertical dotted line); (d) Observed MF (x), completeness-corrected MF (*squares*), background-corrected MF (•) and best fit approximation (solid line).

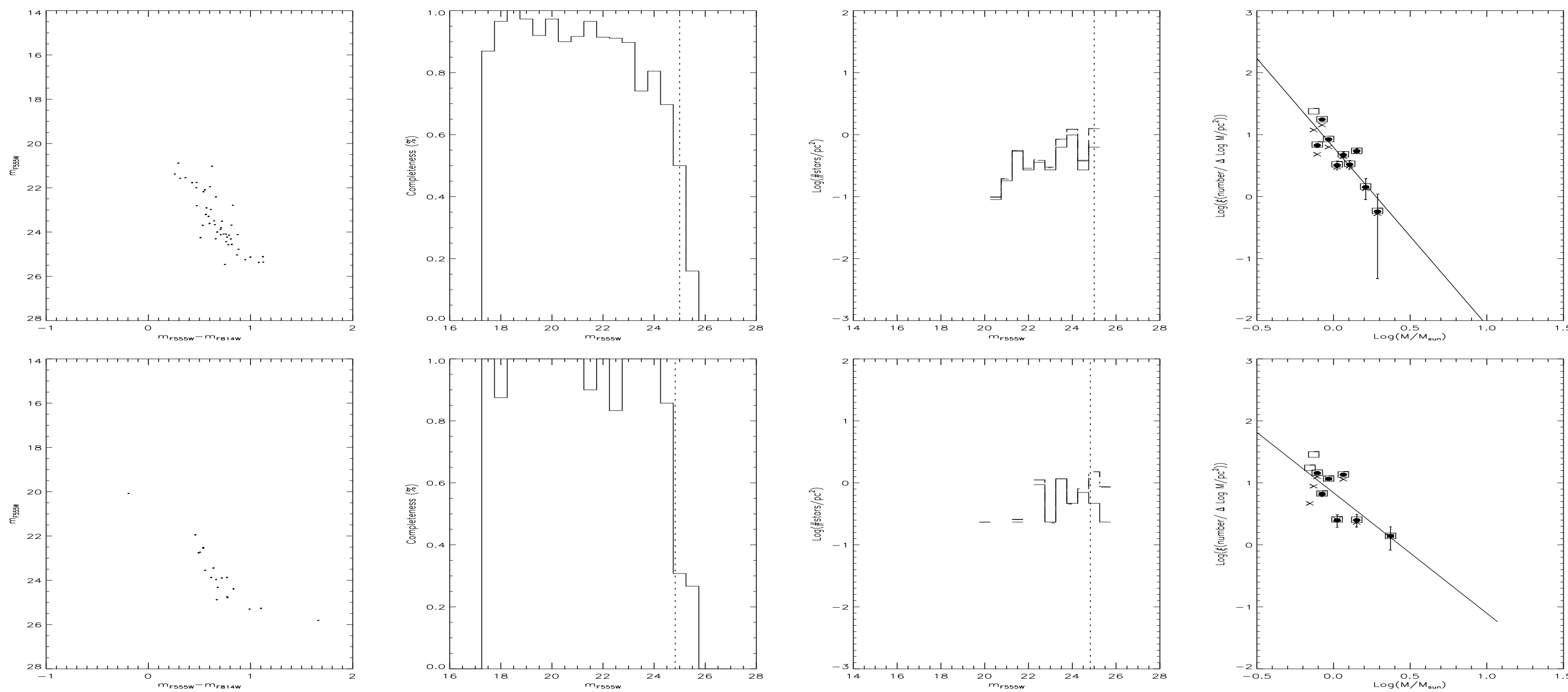

Fig. 17. Diagrams for stars between 120 and 130 arcsec. Each row represents annuli of $10''$. Columns: (a) CMDs for main sequence stars; (b) Completeness diagrams (solid line) and magnitude level for 50% completeness (vertical dotted line); (c) Observed LF (solid line), completeness-corrected LF (dashed line) and background-corrected LF (dash-dotted line)and magnitude level for 50% completeness (vertical dotted line); (d) Observed MF (x), completeness-corrected MF (*squares*), background-corrected MF (•) and best fit approximation (solid line).

creates a steeper IMF due to the lack of massive stars as we move outwards; and in combining them, we see a rapid decrease in the slope of the IMF (very shallow at the core and rapidly decreasing with distance, and flattening in the most outwardly parts as can be seen in Figure 12).

Esteban Silva-Villa acknowledges the Space Telescope Scientific Institute (STScI) for its financial support and hospitality during a stay as a Summer Student (2004) and as an invited astronomer (2005) in Baltimore, where the main part of this work was performed. The authors also thank Luz Angela Cubides for proof reading.

REFERENCES

Bica, E. L. D., Schmitt, H. R., Dutra, C. M., & Oliveira, H. L. 1999, AJ, 117, 238
Claudius, M., & Grosbol, P. J. 1980, A&A, 87, 339
D'Antona, F. 1998, in ASP Conf. Ser. 142, The Stellar Initial Mass Function, ed. G. Gilmore & D. Howell (San Francisco: ASP), 157
Dolphin, A. E. 2000, PASP, 112, 1397
Elson, R. A. W. 1991, ApJS, 76, 185
Holtzman, J. A., Burrows, C. J., Casertano, S., Hester, J. J., Trauger, J. T., Watson, A. M., & Worthey, G. 1995, PASP, 107, 1065
Kalirai, J. S., Fahlman, G. G., Richer, H. B., & Ventura, P. 2003, AJ, 126, 1402
Kennicutt, R. C., Jr. 1998, in ASP Conf. Ser. 142, The Stellar Initial Mass Function, ed. G. Gilmore & D. Howell (San Francisco: ASP), 1
Kroupa, P. 2001, MNRAS, 322, 231
Kroupa, P., & Boily, C. M. 2002, MNRAS, 336, 1188
Kroupa, P., Tout, C. A., & Gilmore, G. 1990, MNRAS, 244, 76
_________. 1993, MNRAS, 262, 545
Lejeune, T., & Schaerer, D. 2001, A&A, 366, 538
Massey, P. 2003, ARA&A, 41, 15
Miller, G. E., & Scalo, J. M. 1979, ApJS, 41, 513
Nota, A. 1999, HST Proposal 8134, Stellar Populations in Clusters
Phelps, R. L., & Janes, K. A. 1993, AJ, 106, 1870
Prisinzano, L., Carraro, G., Piotto, G., Seleznev, A. F., Stetson, P. B., & Saviane, I. 2001, A&A, 369, 851
Prisinzano, L., Micela, G., Sciortino, S., & Favata, F. 2003, A&A, 404, 927
Salpeter, E. 1955, ApJ, 121, 161
Sagar, R., Munari, U., & de Boer, K. S. 2001, MNRAS, 327, 23
Sanner, J., & Geffert, M. 2001, A&A, 370, 87
Scalo, J. M. 1986, Fundam. Cosmic Phys., 11, 1
_________. 1998, in ASP Conf. Ser. 142, The Stellar Initial Mass Function, ed. G. Gilmore & D. Howell (San Francisco: ASP), 201
Sirianni, M., Nota, A., Leitherer, C., De Marchi, G., & Clampin, M. 2000, ApJ, 533, 203
Smecker-Hane, T. A., Cole, A. A., Gallagher, J. S., III, & Stetson, P. B. 2002, ApJ, 566, 239
Sung, H., & Bessell, M. S. 2004, AJ, 127, 1014
Taff, L. G. 1974, AJ, 79, 1280
Tarrab, I. 1982, A&A, 109, 285
van den Bergh, S. 1957, ApJ, 125, 445
Yadav, R. K. S., & Sagar, R. 2002, MNRAS, 337, 133
_________. 2004, MNRAS, 351, 667

E. Silva-Villa and M. Sirianni: Space Telescope Science Institute, 3700 San Martin Drive, Baltimore, MD 21218, USA (E.SilvaVilla@astro.uu.nl, sirianni@stsci.edu).
J. Zuluaga: Instituto de Física, Universidad de Antioquia, A. A.1226, Medellín, Colombia (zuluaga@fisica.udea.edu.co).